

Collisional dissociation of 200–600-keV D_2^+ ions in Ar and H_2 targets

D. Nir, E. Navon, A. Ginzburg, and A. Mann

Department of Physics, Technion—Israel Institute of Technology, Haifa 32000, Israel

(Received 12 October 1982)

We measured all the collisional dissociation channels of D_2^+ in the energy range 200–600 keV in the gas targets H_2 and Ar. The various channels were resolved with the use of an electrostatic deflector into a set of detectors. Rate equations were developed and used in the analyses of the data to extract ratios of cross sections. These ratios of D^+ and D^0 charge-exchange cross sections and D_2^+ dissociation cross section were found to be consistent with those of H_2^+ dissociation at the same velocities. The measurement of the negative fragments shows that there is hardly any direct population of the dissociation channels containing D^- fragments. The negative fragments are formed via a secondary collision of the non-negative fragments formed in the dissociation process.

I. INTRODUCTION

Several works measured the cross sections for the dissociation of D_2^+ (or H_2^+) below the 1-MeV region.^{1–4} The cross sections for charge exchange by atomic hydrogen are also known.^{5–7} In a previous work⁸ it was found that in the energy range 250–600 keV, simple relations exist between the dissociation cross section of H_2^+ and the cross sections for electron exchange. These relations were not studied at lower velocities because of machine limitation. On the other hand, Cisneros *et al.*^{4,9} and Alvarez *et al.*¹⁰ investigated the mechanism of the negative-fragment formation in the dissociation of D_2^+ and D_3^+ only at low energies.

It is the aim of this work to extend and bridge those studies by an investigation of the dissociation of the D_2^+ projectiles in the region of 200–600 keV (corresponding to H_2^+ in 100–300 keV). The measurement of all dissociation fragments and, in particular, the negative fragments and their complements may add detailed information on the formation process of those fragments, and may also give an answer as to whether the simple relation between the dissociation cross section and the electron-exchange cross sections found in the previous work⁸ on H_2^+ is valid at lower velocities or not. The use of D_2^+ is also of interest because the dissociation of D_2^+ in this energy region is one of the promising methods to obtain neutral energetic beams of deuterium atoms for the heating of plasma in fusion reactors.¹¹

In Sec. II we describe briefly the experimental system. In Sec. III we present the experimental results. We show the dependence of the dominant charge states on the target gas and on its pressure and the measurements of negative fragments D^- with their complements as a function of the target gas. In Sec. IV we compare the theory of the dominant charge states⁸ with the results of dissociation at lower energies. We also analyze the formation of D^- fragments and its mechanism and show that these are unlikely to be formed directly in the dissociation.

II. EXPERIMENTAL SYSTEM

The D_2^+ beam in the energy range 200–600 keV was obtained from the Technion J. N. Van de Graaf accelera-

tor. It was directed towards the center of the differential-pumped dissociation chamber in front of the scattering chamber. The width of the beam was 0.3 mm, determined by an aperture at the entrance to the dissociation chamber. The angular spread of the beam was less than 0.1° . Its intensity was reduced to 1000 particles/sec by means of slits before the magnet. A 3- and a 6-mm circular aperture beyond the dissociation chamber permitted fragments scattered at angles up to 1.5° to reach the detectors. The impurities were mainly D^+ and amounted to only a few percent of the beam. More details are available in Refs. 12 and 13. The gas target was either H_2 or Ar and its pressure was measured in the dissociation chamber by a Hastings NV-8 vacuum gauge sensitive in the 1-mTorr region.

The molecular-ion fragments were separated according to their charges by means of a horizontal deflector and measured by a set of detectors. The working voltages were determined empirically by checking the undissociated beam and its dependence on the deflection voltage. A vertical deflector made it possible to carry out during the experiment empirical checks of the accuracy of the height of the various detectors. The fragments were detected by three surface-barrier (SB) detectors each with an active area of 300 mm², whereas the SB detector for the undissociated beam had an active area of 50 mm².

Two energy peaks were usually obtained in each of the large-area detectors, one at the beam energy when both fragments were detected simultaneously and the other at half the beam energy when a single fragment was counted. The signals obtained from the neutral-fragment detector at 0° and those of the D^- fragments at the appropriate detector were analyzed by a multichannel analyzer (MCA) under a coincidence condition with the signal coming from the D^+ and D^0 fragment detectors. The full energy signals at the spectrum of singles were due to the simultaneous detection of two charged D^+ fragments or two D^0 fragments. The signals of the undissociated beam coming from the small detector were also counted in a scaler. This made it possible to distinguish between the undissociated D_2^+ molecules and the five dissociation channels D^-D^0 , D^-D^+ , $2D^0$, D^-D^+ , and $2D^+$. More details of the experimental system and the electronic circuits are available in Refs. 12 and 13.

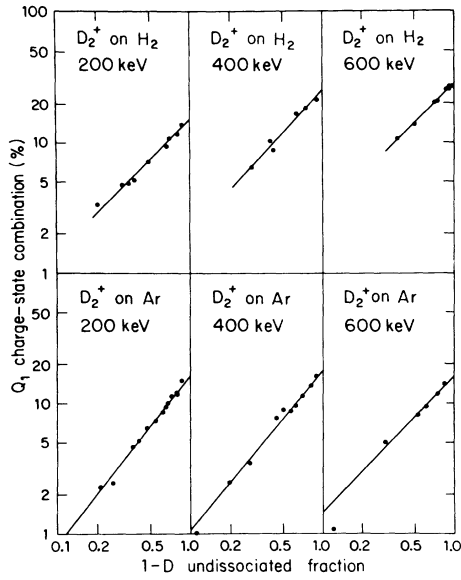


FIG. 1. Charge-state combination Q_1 , defined in Eq. (1) in the text, plotted vs the dissociation fraction D . Target gas and projectile energy are shown in every section of the figure.

III. EXPERIMENTAL RESULTS

A. Method of analysis

Let us denote the exit channels according to the fragments and their charges, e.g., D^0D^+ , $2D^0$, etc. The number of counts in each channel will be denoted by parentheses, i.e., (D^0D^+) , $(2D^0)$, etc. Out of these we calculate the fraction of each dissociation channel, denoted by a square bracket around the dissociation channel, e.g., $[2D^0]$ is the number of $2D^0$ pairs divided by the number of the incoming projectiles D_2^+ . We define the fraction of dissociated molecules as D and therefore the fraction of undissociated molecules is by definition $1-D$. In Appendix A we show that the charge states are well described by an expression which consists of combinations of powers of $1-D$. Therefore certain linear combinations of the charge states are simple powers of $1-D$. We exhibit such quantities,

$$Q_1 = -(\phi_+[D^0] - \phi_0[D^+]) / \ln(1-D) \quad (1)$$

and

$$Q_2 = V_2 + P_2[D_2^+] / \left[1 - 2 \frac{\sigma_c + \sigma_l}{\sigma_d} \right]. \quad (2)$$

Here $[D^0] = [2D^0] + \frac{1}{2}[D^0D^+]$, $[D^+] = [2D^+] + \frac{1}{2}[D^0D^+]$, and ϕ_0 (ϕ_+) is the neutral (charged) fraction at equilibrium of an atomic projectile at the same velocity. In Eq. (2)

$$V_2 = \phi_+^2[2D^0] - \phi_+\phi_0[D^0D^+] + \phi_0^2[2D^+]$$

and

$$P_2 = \phi_+^2 P_{00} - \phi_+\phi_0 P_{0+} + \phi_0^2 P_{++},$$

P_{00} , P_{0+} , and P_{++} are the probabilities for direct popula-

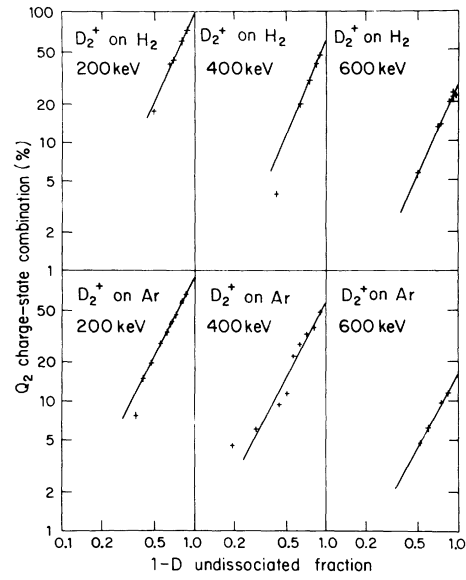


FIG. 2. Charge-state combination Q_2 , defined in Eq. (2) in the text and in Appendix A, plotted here vs the dissociation fraction D . Target gas and projectile energy are shown in every section of the figure.

tion of the corresponding channels in a single collisional dissociation. Q_1 and Q_2 are plotted versus $1-D$ (where D is the dissociation fraction) on a log-log plot in Figs. 1 and 2. According to Appendix A, we can study the relations between the various cross sections from the slopes of these graphs.

The fraction of negative fragments is presented divided by the dissociation fraction for the reason explained below. The fractions of the dominant charge states divided by the dissociation fraction are almost constant up to 50% dissociation.

B. Experimental results for the dominant charge states

Figure 1 shows Q_1 [Eq. (1)] vs $1-D$ on a log-log plot for three energy values and two target gases. The bombarding energy and target gas are indicated in each part of the figure. In the figure we see an approximately linear dependence for all energies and target gases. From the linear graph we extract its slope and the intersection with the $D=0$ axis corresponding to the single-collision regime. The slope is $(\sigma_c + \sigma_l + \sigma_d)/2\sigma_d$ as shown in Appendix A. The intercept of Q_1 with the line $1-D=1$ is P_1 , which is a constant resulting from combinations of the differential equations. This behavior is very similar to that found for H_2^+ fragments in a previous work⁸ and the same results are obtained in the region where the velocities of the ion overlap. In the region of lower velocities there are some deviations which will be discussed below.

Figure 2 exhibits Q_2 [Eq. (2)] vs $1-D$ on a log-log plot and we see here again an approximately linear relationship. The slope of these graphs is $2(\sigma_c + \sigma_l)/\sigma_d$, as is expected from the rate equations and their solution in Appendix A. The intercept value at $1-D=1$ is P_2 , the corresponding constant.

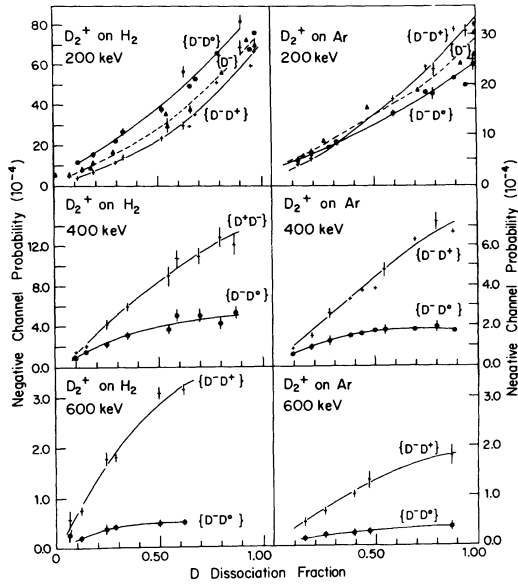


FIG. 3. Shows the probability of D_2^+ dissociation channels containing negative fragments D^- plotted vs the dissociation fraction D . Gas target and projectile energy are indicated in every section of the figure. At D_2^+ energy of 200 keV we also present data of D^- formation by atomic deuterium projectile. For more details see text. Solid and dashed lines are empirical and show the trends of the data. Every line is labeled by the appropriate dissociation channel.

C. Experimental results for negative fragments

Figure 3 shows the results for channels containing D^- fragments. Because the negative fraction rises very fast with D , we present it divided by D ; i.e., we actually present the relative probabilities of obtaining negative fragments in a particular dissociation channel. These relative probabilities are denoted by curly brackets: $\{D^-D^0\} = [D^-D^0]/D$ and $\{D^-D^+\} = [D^-D^+]/D$. The projectile energy and target gas are indicated in the figure. In addition we show in Fig. 3 in the sections of 200-keV projectile energy the probability of obtaining a D^- fragment from a D^+ atomic beam plotted versus the quantity

$$F_0 = \frac{[\Delta^0](p) - [\Delta^0](\infty)}{[\Delta^0](0) - [\Delta^0](\infty)}. \quad (3)$$

F_0 is a measure of the deviation of the neutral fraction $[\Delta^0]$ of atomic beam at target-gas pressure p from its

equilibrium value $[\Delta^0](\infty)$ corresponding to infinite pressure. A more complete treatment of the quantity F_0 is given in Appendix B, and there we show that it is equivalent to the dissociation fraction $1-D$.

In Fig. 3 one sees that the relative probabilities for dissociation channels containing negative fragments rise approximately linearly with D , in variance with the constant value of the relative probabilities of the dominant channels, e.g., D^0D^+ . An example for the linear dependence of the fractions of the dominant channels on D can be seen in Ref. 8.

Furthermore, at 200 keV the probabilities of the two negative channels are approximately equal ($\{D^-D^0\} \cong \{D^-D^+\}$): They also equal the probability of obtaining a D^- from a D^+ beam. We will discuss some conclusions in Sec. IV.

IV. COMPARISON WITH THEORY

A. Dominant channels

In Figs. 1 and 2 we see that the particular combinations Q_1, Q_2 (defined in Appendix A) are simple powers of $1-D$. This is in accordance with Ref. 8 which assumes a primary molecular dissociation process followed by charge-exchange processes of any fragment. Various factors which may cause deviations from this picture, e.g., the influence of the different vibration states or an electron capture and a formation of a D_2^0 molecule, are significant only at the lower bound of our energy region. We will discuss these deviations later. For the prediction of the charge states, however, we ignore them in the calculations which are used to extract cross-section ratios. The results are summarized in Table I.

In Table I P_0 is the probability of obtaining a neutral fragment in a single dissociative collision of D_2^+ . ϕ_0 , the equilibrium probability for a hydrogen projectile to emerge as a neutral atom, is taken from Ref. 14. We note that ϕ_0 changes by a factor of 10 between 200 and 600 keV, whereas $(\sigma_c + \sigma_l)/\sigma_d$ and $P_0 - \phi_0$ hardly change at all. At the lower energy, however, some extracted parameters have different values than at higher energies.

It is clear that specific molecular phenomena such as the vibration states and electron capture without dissociation become more important at low velocities, and one may expect deviations from our simple model. Table I shows that above an energy of 400 keV for a D_2^+ projectile (or 200 keV for H_2^+) one can predict the charge states of the molecular-ion fragments using the rate equations and the extracted parameters in Table I. It is well known

TABLE I. Gives the parameters extracted from the experimental data. ϕ_0 is the equilibrium neutral fraction of D^+ beam in the same gas target and at the same velocity. σ_c is the electron-capture cross section, σ_l the electron-loss cross section, and σ_d is the molecular dissociation cross section. P_0 is the probability for neutral fragment in a single dissociative collision of D_2^+ .

$E_{D_2^+}$ (keV)	ϕ_0	$\frac{\sigma_c + \sigma_l}{\sigma_d}$			$P_0 - \phi_0$
	H ₂	H ₂	Ar	H ₂	Ar
200	0.525	1.02(5)	1.31(7)	0.15(1)	0.16(1)
400	0.183	1.10(5)	1.21(7)	0.25(1)	0.17(1)
600	0.063	0.99(5)	1.04(7)	0.28(1)	0.15(1)

for atomic projectiles that charge-exchange cross sections depend on the ratio of electron orbital velocity and projectile velocity (Bohr's criterion). When the velocity of the projectile electron is lower than the velocity of the projectile, the electron is stripped¹⁵; this is the dominant factor and all other parameters are less important. In this experiment we see that the deviations probably begin when the velocity of the projectile is about the same as the orbital velocity of the molecular electron.

The analysis summed in Table I is not particularly sensitive to effects of the vibration states, which are expected to appear in the single-collision region and not in the pre-equilibrium region. Electron capture and D_2^0 formation without dissociations is a process which is indistinguishable from $[2D^0]$ in our present experimental system; the separation is further complicated since all these fragments are neutral. These two neutral exit channels were once separated in this energy region¹ and the amount of D_2^0 molecular clusters was found to be about 33% of the neutral channel probability. In a measurement made by us we have found similar amounts. One may perform an analysis taking into account the separation of D_2^0 from $2D^0$ and adjoining D_2^0 to the undissociated ions D_2^+ . In such an analysis it was found that the linear dependence remains and the slope is larger than those in Fig. 1, but the change is significant only at 200 keV. The corrected slopes show that the quantity $(\sigma_c + \sigma_l)/\sigma_d$ changes whereas σ_l/σ_d is more likely to be constant equal to 1.0. Further checks of the effect at lower velocities require a different experimental system.

B. Negative-fragments formation

Figure 3 shows that the relative fractions $[D^-D^0]/D$ and $[D^-D^+]/D$ have an approximately linear dependence on D , i.e., the negative fractions are quadratic in D . This dependence suggests a two-step process for D^- formation, because the population of every directly populated dissociation channel is proportional to D at small dissociation fractions.

There are three kinds of two-step processes which may contribute to the formation of negative fragments: (a) collisional excitation without dissociation followed by electron capture and dissociation in a further collision, (b) electron capture without dissociation followed by collisional dissociation of the D_2^0 molecule, and (c) dissociation and additional charge exchange in collisions of the fragments. A molecular quantity which may give more information on the process representing the total probability of forming negative ions is

$$\{D^-\} = \frac{[D^-D^0] + [D^-D^+]}{[D^0] + [D^+]}. \quad (4)$$

This quantity was calculated at 200 keV and compared with $\{\Delta^-\}$, the corresponding probability for an atomic deuterium beam at the same projectile velocity

$$\{\Delta^-\} = [\Delta^-]/([\Delta^0] + [\Delta^+]). \quad (5)$$

As may be seen from Fig. 3 the probability for negative molecular fragments is twice that of an atomic projectile. This is consistent with a two-step process where the negative ions D^- are formed through further collisional charge

exchanges of the dissociation fragments. We do not see possible connections between the other two mechanisms mentioned above and this result. Also the fact that the results do not depend on the target gas is consistent only with the additional charge exchange of the formed fragments.

The ratio between $\{D^-D^0\}$ and $\{D^-D^+\}$ is approximately P_0/P_+ near $D=0$ and approximately ϕ_0/ϕ_+ near $D=1$. Such a result is expected if there is no correlation between the D^- fragment and the complementary fragment, namely, $\{D^-D^0\} = \{D^-\}\{D^0\}$.

The existence of correlation between a negative fragment and its complementary fragment can be shown by comparing two quantities. The first is $[D^-D^0]/([D^-D^0] + [D^-D^+])$ (which is the relative probability for a neutral complementary fragment) and the second is $[D^0]/([D^0] + [D^+])$ (which is the relative probability of neutral fragments). The dependence of these two quantities on the dissociation fraction is different especially at the higher energies, and the former one is decreasing faster with increasing D .

Rate equations for the dissociation were constructed under the assumption of negligible direct formation of D^- in the dissociation. Summing the differential equations for the two channels D^-D^0 and D^-D^+ cancels out the coupling terms and yields

$$\begin{aligned} \frac{d}{dN}([D^-D^0] + [D^-D^+]) \\ = \sigma_{0,-1}[D^0] + \sigma_{1,-1}[D^+] \\ - (\sigma_{-1,1} + \sigma_{-1,0})([D^-D^0] + [D^-D^+]). \end{aligned} \quad (6)$$

$[D^0]$ is the neutral fraction in the dissociation and $[D^+]$ the charged fraction. $\sigma_{0,-1}$, $\sigma_{1,-1}$, $\sigma_{-1,0}$, and $\sigma_{-1,1}$ are the cross sections for charge exchanges involving D^- in the usual notation. For a beam of hydrogen atoms there is a similar rate equation

$$\begin{aligned} \frac{d\{\Delta^-\}}{dN} = \sigma_{0,-1}\{\Delta^0\} + \sigma_{1,-1}\{\Delta^+\} \\ - (\sigma_{-1,0} + \sigma_{-1,1})\{\Delta^-\}. \end{aligned} \quad (7)$$

Here, Δ replaces D to indicate results for atomic projectiles.

In this equation $\{\Delta^-\}$, $\{\Delta^0\}$, and $\{\Delta^+\}$ are the probabilities of the channels and their sum is 1.0, unlike the fractions of dissociation channels which are normalized to the total dissociation fraction D . The similarity of Eqs. (6) and (7) and the same cross sections suggests a relation between the probabilities of D^- formation

$$[D^-D^0] + [D^-D^+] \cong 2D\{\Delta^-\}, \quad (8)$$

which is well satisfied in Fig. 3. If D^- is generated only in a two-step process, this relation can be understood in the following way: The fraction of atomic fragments in the molecular beam is $2D$, consisting of both D^0 and D^+ . The relative quantity of D^0 is not exactly the same as in a D^+ atomic beam, but if the cross sections for D^- formation are similar then the error is small. These experimental data are not sufficient to extract the four charge-exchange cross sections involving D^- . However, it is clear that $\sigma_{1,-1} < \sigma_{0,-1}$, in accordance with the literature

and the difference is increasing with the increase of projectile energy.

V. CONCLUSIONS

In this experiment we have detected all the heavy fragments obtained in the dissociation of D_2^+ . The dependence of their charge states on the dissociation fraction, the bombarding energy, and the target gas was measured. The analysis of the dominant charge states shows that down to 200 keV the charge states may be reproduced by the solutions of the rate equations and the relation $\sigma_d = \sigma_l + \sigma_c$. At the lower energies where the translational velocity of the projectile is about the same as the orbital velocity of the bound electron there are some deviations.

Another important result is that in this energy region the direct population of exit channels containing negative fragments is rather small compared with the probability of obtaining negative fragments in a two-step process. The steps of this process were identified as dissociation followed by a further collisional charge exchange of the fragments.

ACKNOWLEDGMENTS

This work was supported in part by the Israeli Commission for basic research.

APPENDIX A

The rate equations for D_2^+ are similar to those for H_2^+ (Ref. 8) assuming additional charge-exchange collisions for the dissociated fragments,

$$\frac{d[D_2^+]}{dN} = -\sigma_d[D_2^+], \quad (A1)$$

$$\frac{d[2D^0]}{dN} = \sigma_d P_{00}[D_2^+] - 2\sigma_l[2D^0] + \sigma_c[D^0D^+], \quad (A2)$$

$$\frac{d[D^0D^+]}{dN} = \sigma_d P_{0+}[D_2^+] + 2\sigma_l[2D^0] - (\sigma_c + \sigma_l)[D^0D^+] + 2\sigma_c[2D^+], \quad (A3)$$

$$\frac{d[2D^+]}{dN} = \sigma_d P_{++}[D_2^+] + \sigma_l[D^0D^+] - 2\sigma_c[2D^+]. \quad (A4)$$

Here P_{00} , P_{0+} , and P_{++} are the probabilities for direct populations of the corresponding channels in a single dissociation collision, and their sum is very nearly 1.0. The above are four coupled linear differential equations. They

TABLE II. Shows the linear combinations of the fractions of dissociation channels which decouple the differential equations of the process. ϕ_0 is the equilibrium neutral fraction, and $\phi_+ = 1 - \phi_0$.

λ_i	V_i
0	$[2D^0] + [D^0D^+] + [2D^+]$
$\sigma_c + \sigma_l$	$\phi_+[2D^0] + \frac{1}{2}(\phi_+ - \phi_0)[D^0D^+] - \phi_0[2D^+]$
$2(\sigma_c + \sigma_l)$	$\phi_+^2[2D^0] - \phi_+ \phi_0[D^0D^+] + \phi_0^2[2D^+]$

can be solved by taking appropriate linear combinations V_i of $[2D^+]$, $[D^0D^+]$, and $[2D^0]$, which satisfy simple uncoupled equations characterized by eigenvalues

$$\frac{dV_i}{dN} = \sigma_d P_i[D_2^+] - \lambda_i V_i, \quad i = 1, 2, 3. \quad (A5)$$

The λ_i and V_i are summarized in Table II, and the P_i are constants which result from the combinations of Eqs. (9)–(12). $[2D^0] + [D^0D^+] + [2D^+]$ is the combination related to $\lambda=0$ and corresponds to conservation of the number of particles. For $\lambda_1 = \sigma_c + \sigma_l$, when $\sigma_d \cong \sigma_c + \sigma_l$, the differential equation has the solution

$$V_1 = P_1((1-D)^{(\sigma_c + \sigma_l + \sigma_d)/2\sigma_d}) \ln(1-D)$$

and therefore $Q_1 = V_1/\ln(1-D)$ is a power function of $(1-D)$. For $\lambda_2 = 2(\sigma_c + \sigma_l)$ it can be shown that the quantity $Q_2 = V_2 + [P_2/(1-\lambda_2)][D_2^+]$ is a simple power function of $(1-D)$, i.e., $P_2(1-D)^{\lambda_2/\sigma_d}$.

APPENDIX B

The rate equations for an atomic beam composed of D^+ and D^0 projectiles traversing a target gas are

$$\frac{d[\Delta^0]}{dN} = -\sigma_l[\Delta^0] + \sigma_c[\Delta^+], \quad (B1)$$

$$\frac{d[\Delta^+]}{dN} = \sigma_l[\Delta^0] - \sigma_c[\Delta^+]. \quad (B2)$$

$[\Delta^q]$ indicates the fraction of outgoing particles with charge q . These equations are easily solved. We have $[\Delta^0] + [\Delta^+] \cong 1$, and a simple exponential dependence is given by the following combination:

$$F_0 = \frac{[\Delta^0](N) - [\Delta^0](\infty)}{[\Delta^0](0) - [\Delta^0](\infty)} = \exp[-(\sigma_c + \sigma_l)N]. \quad (B3)$$

Using $1-D = \exp(-\sigma_d N)$ we have $F_0 = (1-D)^{(\sigma_c + \sigma_l)/\sigma_d}$ and since $(\sigma_c + \sigma_l)/\sigma_d \simeq 1.0$ F_0 is essentially equal to $1-D$ and one may use it to compare the results for atomic and molecular projectiles.

¹D. R. Sweetman, Proc. R. Soc. London, Ser. A **256**, 416 (1960).

²L. I. Pivovarov, V. M. Tubaev, and M. T. Novikov, Zh. Eksp. Teor. Fiz. **40**, 34 (1961) [Sov. Phys.—JETP **13**, 23 (1961)].

³H. S. W. Massey, E. H. S. Burhop, and H. G. Gilbody, *Electronic and Ionic Impact Phenomena* (Oxford University Press, London, 1974), Vol. 4.

⁴C. Cisneros, I. Alvarez, C. F. Barnett, J. A. Ray, and A.

Russek, Phys. Rev. A **14**, 88 (1976).

⁵H. Tawara and A. Russek, Rev. Mod. Phys. **45**, 178 (1973).

⁶L. H. Toburen, M. Y. Nakai, and R. A. Langley, Phys. Rev. **171**, 114 (1968).

⁷L. M. Welch, K. H. Berkner, S. N. Kaplan, and R. V. Pyle, Phys. Rev. **158**, 85 (1967).

⁸D. Nir, E. Navon, A. Mann, and B. Rosner, Phys. Rev. A **22**,

- 1485 (1980).
- ⁹C. Cisneros, I. Alvarez, R. Garcia, C. F. Barnett, J. A. Ray, and A. Russek, Phys. Rev. A **19**, 631 (1979).
- ¹⁰I. Alvarez, C. Cisneros, C. Barnett, and J. A. Ray, Phys. Rev. A **14**, 602 (1976).
- ¹¹A. Lorentz, Phys. Rep. **37**, 53 (1978).
- ¹²D. Nir, B. Rosner, A. Mann, and D. Maor, Phys. Rev. A **16**, 1483 (1977).
- ¹³D. Nir, A. Weinberg, A. Mann, M. Meron, and S. Gordon, Phys. Rev. A **18**, 1399 (1978).
- ¹⁴S. K. Allison, Rev. Mod. Phys. **30**, 1137 (1958).
- ¹⁵H. D. Betz, Rev. Mod. Phys. **44**, 465 (1972).